

Distinguishing two groups of flavin reductases by analyzing the protonation state of an active site carboxylic acid

Verónica I. Dumit,^{1,2} Néstor Cortez,² and G. Matthias Ullmann^{1*}

¹Structural Biology/Bioinformatics, University of Bayreuth, 95447 Bayreuth, Germany

²Instituto de Biología Molecular y Celular de Rosario, CONICET & Universidad Nacional de Rosario, S2002LRK Rosario, Argentina

ABSTRACT

Flavin-containing reductases are involved in a wide variety of physiological reactions such as photosynthesis, nitric oxide synthesis, and detoxification of foreign compounds, including therapeutic drugs. Ferredoxin-NADP(H)-reductase (FNR) is the prototypical enzyme of this family. The fold of this protein is highly conserved and occurs as one domain of several multidomain enzymes such as the members of the diflavin reductase family. The enzymes of this family have emerged as fusion of a FNR and a flavodoxin. Although the active sites of these enzymes are very similar, different enzymes function in opposite directions, that is, some reduce oxidized nicotinamide adenine dinucleotide phosphate (NADP⁺) and some oxidize reduced nicotinamide adenine dinucleotide phosphate (NADPH). In this work, we analyze the protonation behavior of titratable residues of these enzymes through electrostatic calculations. We find that a highly conserved carboxylic acid in the active site shows a different titration behavior in different flavin reductases. This residue is deprotonated in flavin reductases present in plastids, but protonated in bacterial counterparts and in diflavin reductases. The protonation state of the carboxylic acid may also influence substrate binding. The physiological substrate for plastidic enzymes is NADP⁺, but it is NADPH for the other mentioned reductases. In this article, we discuss the relevance of the environment of this residue for its protonation and its importance in catalysis. Our results allow to reinterpret and explain experimental data.

Proteins 2011; 79:2076–2085.

© 2011 Wiley-Liss, Inc.

Key words: cytochrome P450 reductase; electrostatic calculations; ferredoxin-NADP(H)-reductase; flavoenzyme; oxidoreductase.

INTRODUCTION

Flavin-containing enzymes catalyze a broad spectrum of biochemical reactions involved in important metabolic routes such as oxidative phosphorylation. Their most remarkable feature is the ability to split electrons between obligatory mono- and two-electron transporters, as a consequence of the biochemical properties of their prosthetic group.¹ Most flavoproteins contain either flavin mononucleotide (FMN) or flavin adenine dinucleotide (FAD) as prosthetic group.^{1,2} However, a small number of them contain both cofactors and constitute the family of diflavin reductases.³ Evolutionarily, diflavin reductases originate from a fusion of two ancestral genes coding for a FMN-containing flavodoxin (Fld) and a ferredoxin-NADP(H)-reductase (FNR).^{4,5} Members of this family are cytochrome P450 reductases (CPR), the α -subunit of bacterial sulfite reductase (SiR), methionine synthase reductase (MSR), nitric oxide synthase (NOS), and the cytoplasmic novel reductase 1 (NR1).⁶

CPR, the most extensively characterized of these enzymes, is found in the endoplasmic reticulum of most eukaryotic cells. It is an integral component of the mono-oxygenase system transferring electrons from NADPH to cytochromes P450 (CYPs) via the FAD and FMN cofactors.⁶ CYPs are involved in the synthesis of endogenous compounds such as steroids, fatty acids and prostaglandins and in the detoxification reactions of foreign compounds including therapeutic drugs. In each catalytic cycle, CYPs must be restored to their reduced state by a CPR.⁷ In addition to its normal physiological functions, CPRs play a role in the reductive activation of many therapeutically important anticancer agents.³ CPRs are also involved in detoxification metabolism of *Trypanosoma cruzi*, the parasite responsible for the trypanosomiasis

Abbreviations: BenC, benzoate-1,2-dioxygenase reductase; CPR, cytochrome P450 reductase; CYP, cytochrome P450; Fd, ferredoxin; Fld, flavodoxin; FNR, plastidic ferredoxin-NADP(H)-reductase; FPR, bacterial ferredoxin-NADP(H)-reductase; MC, Monte Carlo; MSR, methionine synthase reductase; NOS, nitric oxide synthase; NR1, cytoplasmic novel reductase 1; PDR, phthalate dioxygenase reductase; SiR, sulfite reductase; TR, Tanford-Roxby.

Grant sponsor: Deutsche Forschungsgemeinschaft; Grant number: UL 174/7-1; Grant sponsor: Deutscher Akademischer Austauschdienst.

*Correspondence to: G. Matthias Ullmann, Structural Biology/Bioinformatics, University of Bayreuth Universitätsstr. 30, BGI, 95447 Bayreuth, Germany. E-mail: matthias.ullmann@uni-bayreuth.de

Received 8 December 2010; Revised 8 February 2011; Accepted 25 February 2011

Published online 21 March 2011 in Wiley Online Library (wileyonlinelibrary.com).

DOI: 10.1002/prot.23027

known as Chagas' disease. *T. cruzi* is refractory to known antiprotozoal agents, and overexpression of CPRs in *T. cruzi* epimastigotes increases its resistance to the typical chemotherapeutic agents.⁷

NOS is the enzyme responsible for NO production. Its C-terminal domain belongs to the diflavin reductase family.⁸ NO acts in key physiological processes including neurotransmission, blood pressure regulation, and the immune response. Deregulation of NO synthesis is associated with diverse human pathologies including immune diabetes, stroke, inflammatory bowel disease, rheumatoid arthritis, hypertension, arteriosclerosis, and infection susceptibility.⁸

MSR is the enzyme responsible for reducing methionine synthase. A large number of cancer cell lines are unable to grow in medium in which methionine is replaced by its precursor homocysteine. Thus, methionine restriction has been considered as a potential cancer therapeutic strategy.⁹

Another diflavin reductase is NR1, which appears widely expressed in human cancer cell lines and could play a potential role in the (de)activation of drugs used in cancer therapy.³ It binds FMN, FAD, and NADPH cofactors and shares about 44% similarity with human CPR, and its sequence arrangement indicates that NR1 is structurally similar to CPR. NR1 supports the metabolism of some antineoplastic agents, and it is thought to be involved in methionine synthesis; however, its precise biological role is unknown.³

FNRs from plants and those from bacteria (FPRs) are monomeric enzymes harboring one molecule of FAD as prosthetic group. FNR in chloroplasts and cyanobacteria oxidize reduced ferredoxin (Fd) to provide the NADPH necessary for CO₂ assimilation. In bacteria, FPRs reduce Fd or Fld with electrons received from NADPH. The reaction is the same as in plants but it occurs in the opposite direction.¹ All FNRs and FPRs have a remarkably similar tertiary structure. The FNR domain of the diflavin reductases resembles this structure. The active site around the FAD in all flavin and diflavin reductases is structurally very similar and contains three highly conserved residues: a cysteine, a serine and a carboxylic acid. The latter is a glutamate in FNRs and FPRs, whereas it is an aspartate in diflavin reductases. The diflavin reductases and FPRs share the direction of the physiological reaction they catalyze and display similar catalytic rates, but according to their tertiary structure, diflavin reductases are more related to FNRs, including the binding mode of the cofactor (Fig. 1).

In this work, we find through electrostatic calculations and analysis of protonation behavior of titratable residues that a highly conserved carboxylic acid in the active site of flavin and diflavin reductases is protonated in FPRs and diflavin reductases but deprotonated in FNRs, at neutral pH. The relevance of this residue in the catalytic mechanism is discussed. Our results can explain previous experimental data.

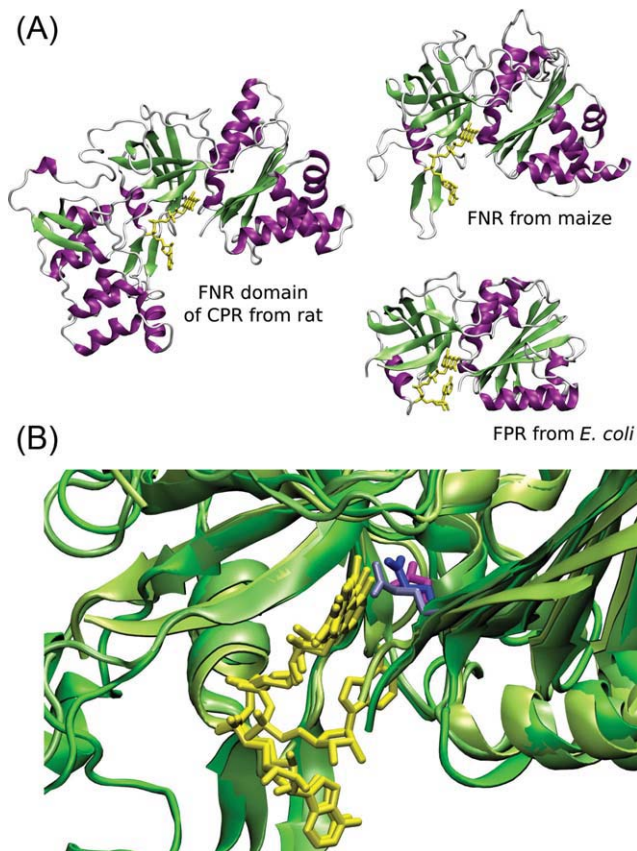


Figure 1

(A) Comparison of the FNR from maize, FPR from *E. coli*, and FNR domain of CPR from rat liver. α -Helices are shown in purple, β -sheets in green, and the rest of the protein in white. The FAD cofactor is displayed in yellow. (B) Degree of exposition of the carboxylic acid and positioning of the cofactor in the active site of CPR from rat, FNR from maize, and FPR from *E. coli*. Proteins were superimposed, and the carboxylic acid in the active site is highlighted: Asp675 from CPR in magenta; Glu312 from FNR in gray; and Glu245 from FPR in blue. Superposition was done using the program MultiProt¹⁰ and the picture was prepared using the program VMD.¹¹

METHODS

Structures for electrostatic calculations

The enzymes used in this work were chosen on the basis of a Dali search¹² using the structure of CPR from rat liver (PDB code: 1amo) as starting point. The reductases as ordered by similarities to the CPR from rat liver are CPR from rat liver and yeast, NOS from rat brain, human MSR, SiR from *Escherichia coli*, FNRs from pea, spinach, paprika, *Anabaena*, maize (leaf and root isoforms), *Leptospira interrogans*, *Plasmodium falciparum*, an iron-sulfur flavoprotein benzoate-1,2-dioxygenase reductase (BenC) from *Acinetobacter sp.*, FPRs from *E. coli*, *Azotobacter vinelandii*, an iron-sulfur flavoprotein phthalate dioxygenase reductase (PDR) from *P. cepacia*, and FPRs from *Pseudomonas aeruginosa*

Table IProtonation Energetics of the Carboxylic Acid in the Active Site of the FNR Domain of Flavin- and Di-Flavin-Reductases, Calculated at pH 7 (kcal mol⁻¹)

PDB ID	Enzyme	Residue	$\Delta G_{TR,7}$	$\Delta\Delta G_{Born}$	$\Delta\Delta G_{back}$	$\Delta G_{TR,7}^{inter}$	pK _{TR,7}	In Figure 2
1amo ¹³	CPR, rat liver	D675	-1.9	-10.9	4.2	-0.7	8.4	(A)
2bn4 ¹⁴	CPR, yeast	D689	-4.7	-7.7	0.3	-1.4	10.4	(A)
1tl1 ⁸	NOS, rat brain	D1393	-3.0	-7.7	0.8	0.2	9.2	(A)
Model	FNR-domain CPR ^{a,b}	D675	-0.1	-9.1	3.0	-2.1	7.1	(B)
1f20 ¹⁵	NOS, rat brain ^b	D1393	0.6	-9.9	2.4	4.0	6.6	(B)
2qtl ¹⁶	MSR, human ^b	D695	-0.7	-7.3	0.4	2.1	7.5	(B)
1ddg ¹⁷	SiR, <i>E. coli</i> [†]	D597	0.9	-4.5	1.5	-0.2	6.4	(B)
1gq0 ¹⁸	FNR, pea	E306	0.8	-3.9	0.9	0.2	6.4	(C)
1fnb ¹⁹	FNR, spinach	E312	0.9	-6.6	3.5	0.4	6.3	(C)
1sm4 ²⁰	FNR, paprika	E360	2.2	-1.9	0.4	0.2	5.4	(C)
1que ²¹	FNR, <i>Anabaena</i>	E301	-2.2	-6.5	1.7	-0.9	8.6	(C)
1gaw ²²	FNR, maize	E312	2.0	-2.2	0.2	0.4	5.6	(C)
1jbg ²³	FNR, maize root	E314	1.9	-2.7	0.6	0.5	5.6	(C)
2rc5 ²⁴	FNR, <i>L. interrogans</i>	E312	3.0	-1.9	0.8	0.6	4.8	(C)
2ok8 ²⁵	FNR, <i>P. falciparum</i>	E314	2.1	-4.3	1.7	1.1	5.4	(C)
1krh ²⁶	BenC, <i>Acinetobacter sp.</i> ^c	E333	-5.8	-7.8	-0.3	-1.2	11.2	(D)
1fdr ²⁷	FPR, <i>E. coli</i>	E245	-4.5	-9.0	0.7	0.2	10.3	(D)
1a8p ²⁸	FPR, <i>A. vinelandii</i>	E252	-6.7	-10.7	1.1	-0.7	11.9	(D)
2pia ²⁹	PDR, <i>B. cepacia</i> ^c	E223	-6.6	-10.2	1.5	-1.5	11.8	(D)
2qdx ³⁰	FPR, <i>P. aeruginosa</i>	E252	-6.8	-10.3	2.5	-2.6	12.0	(D)
2bgj ³¹	FPR, <i>R. capsulatus</i>	E264	-6.4	-10.2	0.9	-0.6	11.7	(D)
Model	Mutant S457A CPR ^a	D675	-7.0	-9.3	2.3	-4.2	12.1	(E)
Model	Mutant C630A CPR ^a	D675	-3.4	-9.5	4.3	-2.4	9.5	(E)

The meaning of the energy contributions is explained in the *Methods* section.^aModeled based on 1amo.^bFNR domain.[†]Iron-sulfur flavoprotein.

and *Rhodobacter capsulatus* (see Table I for PDB codes). Table I follows this order.

Hydrogens were placed using the HBUILD³² routine of CHARMM.³³ The energy of the resulting structures was minimized keeping all nonhydrogen atoms at fixed positions. For this optimization, all titratable groups were in their standard protonation form, for example, acids (aspartate, glutamate, and C-terminus) were deprotonated and bases (arginine, cysteine, histidine, lysine, tyrosine, and resolved N-termini) were protonated. All water molecules and sulfate ions were removed from the structures after the modeling. If the N-terminus was not resolved crystallographically, we blocked the first resolved residue by an acetate group. The unresolved terminus should affect the titration behavior of the rest of the protein only marginally, because it is highly flexible, well solvated, and its charges are consequently well shielded.

Models of CPR

Based on the crystal structure of the CPR from rat liver (PDB code 1amo), three models were build: S457A and C630A mutant CPRs and the FNR-domain from CPR. For the S457A mutant CPR, the atom OG from the serine residue 457 was deleted from the original file and the rest of

the side chain was conserved. The same approach was used to build the C630A mutant CPR: the atom SG from cysteine residue 630 was deleted and the remaining side chain was kept. To construct the model of the FNR domain of CPR, the residues from the N-terminus up to the residue 244, as well as the FMN coordinates, were deleted.

Atomic partial charges

Partial charges of the flavin cofactors, FAD and FMN, and iron-sulfur center of Fd domains were obtained as described before.³⁴ The iron-sulfur center of Fd and the isoalloxazine ring of the flavins were included in oxidized charge forms. We considered two charge forms for all arginine, aspartate, glutamate, lysine, tyrosine, and non-iron coordinating cysteine. The charges for the protonated form of glutamate and aspartate and the deprotonated form of lysine and arginine were symmetrized. Four charge forms were used for the histidine side chain (doubly protonated, ϵ -protonated, δ -protonated, and deprotonated).

Theoretical framework for the computation of protonation probabilities

Protonation probabilities were obtained by combining Poisson-Boltzmann electrostatic calculations with Me-

tropolis Monte Carlo (MC) titrations. The underlying theory is described in detail elsewhere.^{35,36}

For multiprotic systems, a pK_a value can often not be attributed to a single group.^{37,38} Instead, a protonation probability curve can describe the behavior of a group over the whole investigated pH range. However, this curve can deviate substantially from a Henderson-Hasselbalch curve. The theoretical framework used here allows to compute average interaction energies from the protonation probabilities obtained by the MC procedure.^{35,36} The mean-field energy $G_{TR}^\circ(j_k, \text{pH})$ of a particular titratable site j in its protonation form k (p for protonated and d for deprotonated) at a certain pH can be described by its intrinsic energy $G_{intr}(j_k)$ and its average interaction energy, G_{inter} ^{39,40}.

$$G_{TR}^\circ(j_k, \text{pH}) = G_{intr}(j_k) + \sum_{l \neq j}^{N_{site}} \sum_m^{N_{form,l}} G_{inter}(j_k, l_m) p(l_m, \text{pH}). \quad (1)$$

The average interaction energy is the sum over all protonation forms m of all other sites l weighted by the probability p of form l_m at a given pH, $p(l_m, \text{pH})$ that we obtain from a MC calculation. Here, the number of sites of the system is given by N_{site} , and the number of protonation forms of site l is given by $N_{form,l}$.

The averaging of this mean-field approach follows a similar spirit as the calculation of protonation probabilities based on the iterative scheme of Tanford and Roxby (TR).^{41,42} Therefore, we call the pK_a values calculated based on the average interaction energies as Tanford-Roxby- pK_a values:

$$pK_{a,TR}(j, \text{pH}) = -\frac{1}{RT \ln 10} (G_{TR}^\circ(j_p, \text{pH}) - G_{TR}^\circ(j_d, \text{pH})). \quad (2)$$

However, $pK_{a,TR}$ values are pH dependent. The free energy to protonate a site at a given pH can be estimated from this $pK_{a,TR}$ by

$$G_{TR}(j, \text{pH}) = RT \ln 10 (\text{pH} - pK_{a,TR}(j, \text{pH})). \quad (3)$$

This energy is positive if the group is likely to be deprotonated and negative if the group is likely to be protonated. Thus, from this energy it can be seen how easily a group deprotonates or protonates at a given pH.

The intrinsic energy $G_{intr}(j_k)$ of a form j_k is composed of three contributions:

$$G_{intr}(j_k) = G_{model}(j_k) + \Delta G_{Born}(j_k) + \Delta G_{back}(j_k). \quad (4)$$

The model energy $G_{model}(j_k)$ represents the energy of form j_k inside a model compound in solution, which is usually determined experimentally. The Born energy difference $\Delta G_{Born}(j_k)$ characterizes the energy difference for

polarizing the solvent around the protein and the model compound when the site j is charged from zero to its final charge in the protonation form j_k . The background energy difference $\Delta G_{back}(j_k)$ describes the interaction energy difference of form j_k with the charges of atoms not belonging to any site in the protein and in the model compound. The average interaction energy difference at a given pH is

$$\Delta G_{TR, \text{pH}}^{\text{inter}} = \sum_{l \neq j}^{N_{site}} \sum_m^{N_{form,l}} (G_{inter}(j_p, l_m) - G_{inter}(j_d, l_m)) \times p(l_m, \text{pH}). \quad (5)$$

Computation of protonation probabilities and interaction energies

The electrostatic energies represented by the intrinsic energies $G_{intr}(j_k)$ and the interaction energies $G_{inter}(j_k, l_m)$ were calculated by programs based on the MEAD package.^{36,43} The intrinsic energy values are calculated relative to experimentally determined pK_a values of appropriate model reactions of monoprotic compounds in aqueous solution.³⁵ All residues of the types arginine, aspartate, glutamate, lysine, tyrosine, and histidine were considered titratable. The energetic parameters for calculating the protonation were obtained from Poisson-Boltzmann calculations. A dielectric constant of $\epsilon_p = 4$ was assigned to the interior of the protein. This value is used in many studies and enables a reliable prediction of the titration behavior of buried and active site residues.^{44–51} The solvent was modeled as a medium with a dielectric constant of $\epsilon_s = 80$. An ionic strength of $I = 100$ mM and a temperature $T = 300$ K were used. An ion exclusion layer of 2 \AA and a solvent probe radius of 1.4 \AA defined the excluded volume of the protein. The electrostatic potential was calculated using a grid of $131 \times 131 \times 131$ points with two focusing steps at a resolution of 1.0 \AA and 0.2 \AA . The larger grid was geometrically centered on the molecule or complex, whereas the finer grid was geometrically centered on the group of interest.

The probabilities of all protonation forms j_k as a function of pH were calculated by a Metropolis MC algorithm.⁵² The pH was varied from 0 to 14 in steps of 0.2 pH units. For every pH step, the MC calculation consisted of 100 equilibration scans and 10,000 production scans at $T = 300$ K. In one scan, each site of the protein is touched once on average.

RESULTS AND DISCUSSION

Since the first crystallographic structure of spinach FNR was resolved, the conserved carboxylate residue (a glutamate in FNRs and FPRs) in the active site was suggested to be responsible for donating protons to FAD during reduction through a conserved serine residue.¹⁹

Moreover, the conserved glutamate assumes a different position in maize FNR when complexed with Fd suggesting an active role in catalysis.²² The hypothesis that this residue is acting as proton donor was investigated in two experimental systems: FNR from *Anabaena*⁵³ and from spinach⁵⁴; however, no definite conclusion could be reached. Through electrostatic calculations on maize FNR, we could show that this residue has an important role throughout the whole catalytic cycle.³⁴ It was noted, from comparison of the crystal structure of spinach FNR with the one from PDR,¹⁹ that the carboxylate in FNR forms a hydrogen bond to a conserved serine, but it does not in PDR, an iron-sulfur flavoprotein containing a FNR-like domain.²⁹ In this work, we studied the titration behavior of the conserved carboxylate in the active site of all FNRs, FPRs, and diflavin reductases whose crystallographic structure was resolved. Two iron-sulfur flavoproteins, BenC and PDR, that are structurally very similar to the flavin reductases were included. PDR is a fusion protein of a Fd domain and a FNR domain; the latter domain possesses FMN and not a FAD as prosthetic group. Its physiological substrate is NADH, which reduces the FMN and then the Fd domain.²⁹ BenC contains a Fd domain and a FNR domain that binds a FAD molecule. Its substrate is NADH, and it is involved in aerobic biodegradation of aromatic compounds.²⁶ In the analysis, we concentrate particularly on the proton binding behavior of the highly conserved carboxylate in the active site of the FNR domain.

Knowing the protonation of active site residues is crucial for understanding the catalytic mechanism of enzymes. We would like to emphasize that it is not possible to assign a pK_a value to an individual site in molecules like proteins that have strongly interacting titratable groups. As explained in detail in a previous publication,⁴⁰ each site is associated to many microscopic pK_a values. At different pH values, different microstates dominate the ensemble, and thus, different pK_a values are relevant for the titration behavior of the residues. For this reason, the effective pK_a value of a site is pH dependent. For discussing enzymatic mechanisms, protonation energies are however more relevant than pK_a values. For that reason, we are normally discussing protonation energies at pH 7, the physiological pH. A positive value indicates that the group is deprotonated, and a negative value indicates that the group is protonated. The magnitude of the value shows how easy it is to protonate or deprotonate the site.

Influence of the conserved carboxylate residue on the direction of the reaction and on NADP(H) binding

Flavin reductases considered herein can be subdivided in two groups. The first group includes enzymes whose physiological function comprises the transfer of hydride

from NADPH to the FAD (i.e. all diflavin reductases, iron-sulfur flavoproteins, and FPRs). The second group gathers all the enzymes whose physiological function is to reduce NADP^+ with the electrons coming from Fd_{red} (i.e., FNRs). Another characteristic of the second group is the high catalytic efficiency, which is required for the photosynthetic metabolism. The subdivision of these two groups correlates with the titration behavior of the conserved carboxylate of the active site. In the first group, this residue is protonated at pH 7, and in the second group, this residue is deprotonated (Table 1).

Remarkably, the protonation energy of the acidic residue in the active site of FPRs and iron-sulfur flavoproteins at pH 7 is always more negative than $-4.5 \text{ kcal mol}^{-1}$, whereas it is -3 kcal mol^{-1} on average for the equivalent residue in diflavin reductases. All these enzymes catalyze the electron transfer from the NADPH to the isoalloxazine ring as first step in their catalytic reaction.

The second group includes all FNRs, where the protonation energy at pH 7 of the glutamate in the active site is on average 2 kcal mol^{-1} , and thus indicates that the residue is deprotonated. All the enzymes in this second group catalyze the electron transfer from reduced Fld or Fd to the NADP^+ , that is, the opposite reaction than the enzymes in the first group. An exception is the FNR from *Anabaena*, which is able to catalyze reaction in both directions depending on the cell where it is located. In vegetative cells, that is, photosynthetically active, the direction of the reaction corresponds to the one catalyzed by plastidic FNRs, whereas in heterocysts, it is involved in N_2 fixation, and the opposite direction is catalyzed.⁵⁵ In this FNR from *Anabaena*, the protonation energy of the carboxylate is -2 kcal mol^{-1} , and thus, the residue is protonated.

The FNRs that catalyze the reaction in the direction of reducing Fd, as it is the case for FNR from maize root, seem to have evolved from a leaf isoform being then incorporated in metabolic pathways different from photosynthesis. A similar evolution is expected for the FNRs from the parasites *P. falciparum* and *L. interrogans*, as the FNR reaction in these organisms does not yield reducing equivalents for carbon fixation but reduces Fd. However, it is thought that these enzymes were incorporated from plants as a result of a lateral gene transfer.⁵⁶ The grouping of the flavin reductases according to the protonation probability of the active site carboxylate agrees with the classification for FNR and FPR proposed by Ceccarelli *et al.*⁵⁶

It is plausible that evolution has tuned the protonation probabilities of the carboxylate in the active site of flavin reductases to recruit FNR to photosynthesis, which requires high catalytic rates. Moreover in photosynthesis, the catalyzed reaction occurs in the reverse direction when compared with the reaction catalyzed by the other related enzymes. We think that the glutamate is a key

residue to achieve this reversion. In a previous study, we found that a glutamate residue in the active site of FNR changes its protonation state several times to accomplish key functions such as FAD semiquinone stabilization, favoring complex formation with reduced Fd, and hydride transfer from FADH₂ to NADP⁺.³⁴ In addition to these functions, the protonation of the carboxyl group in the active site has a direct consequence for the catalytic cycle of the enzymes. The negatively charged glutamate of FNRs is in a proper position to interact with the positive charge on the nicotinamide ring of the NADP⁺. It has been experimentally observed that the negative charge on the glutamic acid in the active site of plastidic FNR is necessary for proper binding of NADP⁺.⁵⁴ The lack of charge on the equivalent residue in bacterial FPRs and diflavin reductases may disfavor NADP⁺ over NADPH binding. In this way, the reductases would display higher affinity for its physiological substrate and, consequently, higher enzyme efficiency.

Experimental evidence supporting our proposal was obtained through differential spectroscopy. Hubbard *et al.*⁵⁷ observed no peak at 510 nm in difference absorbance spectra and thus concluded that the interaction of the NADP⁺ with isoalloxazine ring of CPR is negligible. They obtained a difference spectrum quite similar to that for wild-type FNR from *Anabaena* when the nucleotide is bound.⁵⁸ The peak at 510 nm in the difference spectra appears when the nicotinamide moiety of NADP⁺ stacks with the isoalloxazine ring of the flavin.⁵⁹ Thus in CPR and FNR from *Anabaena*, the stacking configuration of the nicotinamide moiety of NADP⁺ and the isoalloxazine ring is not favored, presumably due to the lack of the negative charge on the active site carboxylate. In the FNRs in which the carboxylate is negatively charged according to our calculations, the peak at 510 nm in the difference spectra is observed, and thus, nicotinamide moiety of NADP⁺ stacks with the isoalloxazine ring.^{54,59} It is worth mentioning that the FPR from *R. capsulatus* shows a peak at 510 nm in the difference spectrum,⁶⁰ even though our calculations indicate that the active site glutamate is protonated and thus should behave like the FNR from *Anabaena* or CPR regarding the interaction with the oxidized nucleotide. However, FPR from *R. capsulatus* has no aromatic residue stacking the isoalloxazine ring of the flavin that needs to be displaced by the nicotinamide ring to allow stacking. Hence, the active site geometry has less restrictions to allow contact between the isoalloxazine ring and the nicotinamide ring.

A mutation by which the active site glutamate of *Anabaena* FNR was replaced by alanine does not influence the NADP⁺ binding.⁵³ According to our calculations, the glutamate in this enzyme is likely to be protonated, and thus, in agreement with our proposal, its mutation should not strongly bind NADP⁺. However, in FNRs from plants, the glutamate in the active site is negatively charged and its replacement by alanine affects the NADP⁺ binding,⁵⁴

showing that the negative charge on the carboxylic acid in the active site has an influence on the binding of NADP⁺. The mutant enzyme exhibited a decrease of affinity for NADP⁺ to one third of its value in the wild type.⁵⁴ The lack of charge on the carboxylic acid in the diflavin reductases and FPRs does not favor the interaction with NADP⁺, and thus, NADPH is more likely to be bound. This behavior was also observed through the experimental estimation of the inhibition constants of NADP⁺ for mutant and wild-type forms of CPR.⁶¹

Factors affecting the protonation behavior

Figure 1(B) depicts an example of the geometrical arrangement of the carboxylate environment in each group of enzymes. In the FNR, the glutamate is more exposed to the solvent giving rise to a less negative change in the solvation energy (ΔG_{Born}), as the environment with a higher dielectric constant (water) better stabilizes the negative charge on the residue. In the case of FPR and the diflavin reductases, the carboxylate is more buried inside the protein leading to a more negative ΔG_{Born} .

An important finding resulting from the comparison between the structures of wild-type CPR from rat and of mutant forms complexed to NADP⁺ revealed a noticeable mobility of the Fld-domain.⁵⁷ Even a higher mobility of the Fld-domain was noticed when the SiR from *E. coli* was crystallized and the Fld-domain remained unresolved.¹⁷ This conformational flexibility of the Fld domain may be an essential part of the catalytic mechanism. It was suggested that these conformational changes could tune the redox properties of the flavins by altering the environment of the isoalloxazine rings to meet the needs of the individual catalytic steps.^{6,17} To evaluate the influence of the Fld domain on the titration properties of the aspartic acid in the active site of CPR from rat, we modeled the FNR domain for the protein in the absence of the Fld domain by removing the residues from the N-terminus up to residue 244. We calculated the protonation probabilities of this model and of some other diflavin reductases, for which only the FNR domain was crystallographically resolved. Deletion of the Fld domain leads to an increase of the protonation energy such that the residue titrates in the neutral pH range (Table I). From these calculations, we concluded that the Fld domain lowers the protonation energy of the carboxylate by about 1.8 kcal mol⁻¹ at pH 7.

Figure 2(B) shows the titration curves of the active site carboxylates in the FNR domains of the diflavin reductases in the absence of the Fld domain. The shift of these curves to the left in relation to those in Figure 2(A) shows that the protonation probability of the aspartate in the active sites is lower indicating the influence of the Fld domain in burying the carboxylate. Interestingly, the titration curves are still considerably shifted toward

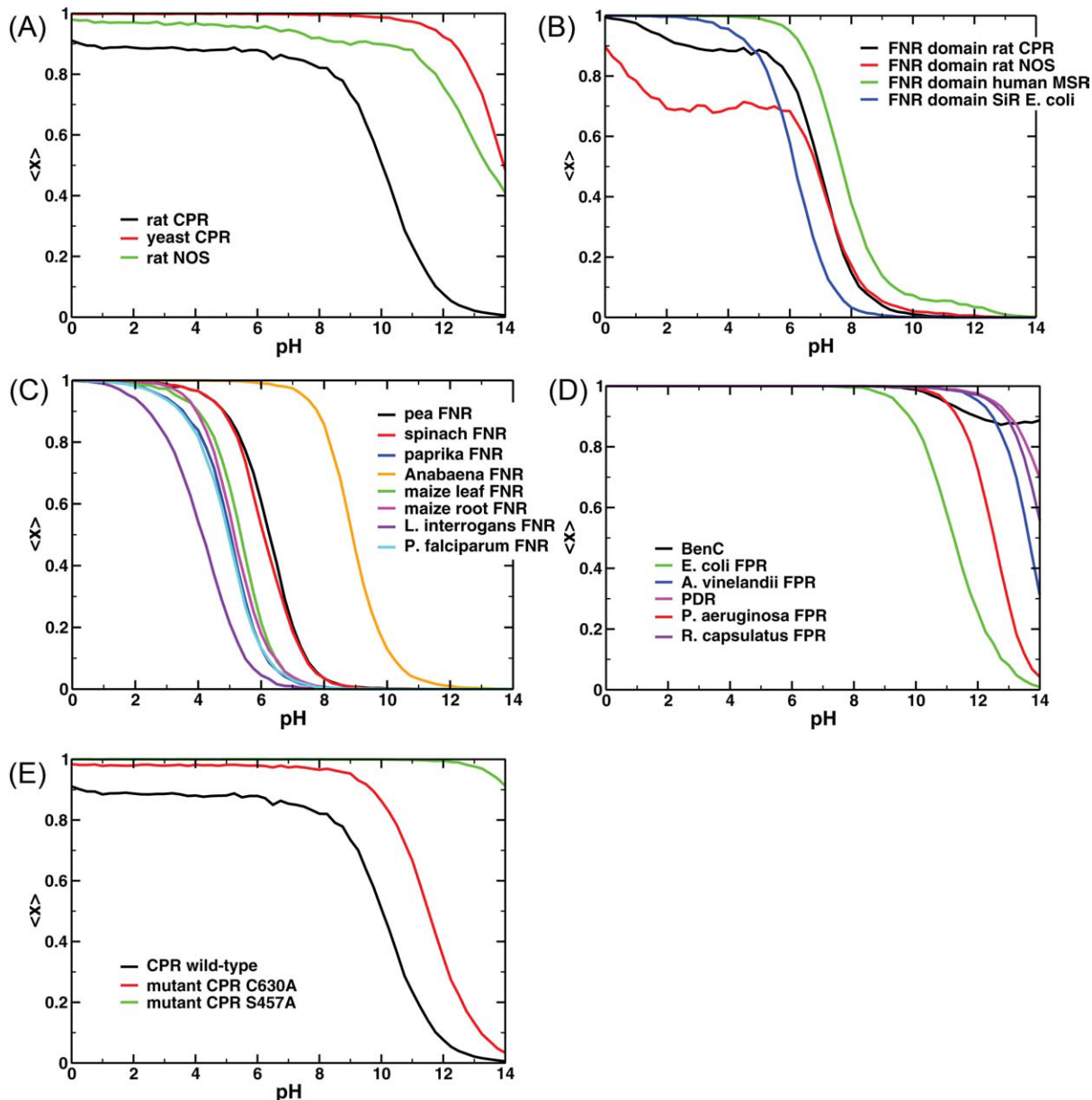


Figure 2

Titration curves. (A) Diflavin reductases: CPR from rat and yeast, and rat NOS; (B) FNR domain from diflavin reductases; (C) FNRs; (D) BenC, FPRs, and PDR; (E) different forms of CPR from rat: wild type, mutant C630A, and mutant S457A.

higher pH when compared with free aspartate. The carboxylate in diflavin reductases is always an aspartate. In solution, the aspartate as model compound has a pK_a of 4.0 leading to a protonation energy of $4.1 \text{ kcal mol}^{-1}$ at pH 7. Thus, the active site of diflavin reductases without the Fld domain lowers the protonation energy by at least $3.2 \text{ kcal mol}^{-1}$ at that pH which favors its protonation. The position of the Fld domain strongly influences the catalytic cycle by forcing the acidic residue to behave in certain steps as proton donor as we already suggested for the glutamate in FNR from maize.³⁴

Proteins with residues that show a highly shifted titration behavior are rare, but not unheard of. For instance, the residues Asp96 and Asp115 in bacteriorhodopsin titrate only when bacteriorhodopsin unfolds at about pH 11–12.⁶² Other proteins with residues displaying unusual titration behavior are for instance the photosynthetic reaction center⁶³ or cytochrome c oxidase.⁶⁴ Usually, residues that are functionally relevant show such a shifted titration behavior. Therefore our findings support an involvement of this highly conserved carboxylate in the mechanism of the flavin reductases.

Effect of mutations on the catalytic mechanism of CPR: Comparison with experimental results

Shen *et al.*,⁶¹ have studied the role of Ser457, Asp675, and Cys630 in CPR from rat. These residues were chosen based on their proximity to the isoalloxazine ring of FAD. It was concluded that these three residues are important for the hydride transfer from NADPH to FAD during catalysis. Cys630 would function in addition as a proton donor/acceptor to the FAD. Substitutions of residues Ser457, Asp675, and Cys630 produced large decreases in k_{cat} with no significant changes in K_m^{NADPH} , indicating that these mutations affect only catalysis but not cofactor binding.

The pH dependence of k_{cat} was also studied in Ref. 61: wild-type k_{cat} displayed $\text{p}K_a$ values of 6.9 and 9.6. The S457A mutant displayed the same acidic $\text{p}K_a$ (6.8), but the $\text{p}K_a$ of the basic group was not seen in the tested pH range. Notably, the acidic $\text{p}K_a$ value of 6.9 was not eliminated by mutation of Asp675. Therefore, it was suggested that some group other than Asp675 is responsible for this $\text{p}K_a$. However, in the mutants of Asp675, the basic $\text{p}K_a$ value was shifted to values >10 . The substitution of Cys630 did not eliminate the acidic $\text{p}K_a$ value but shifted it to 7.8, indicating that although Cys630 is not the ionizable group, it influences the $\text{p}K_a$ value of residue responsible for the pH dependence of k_{cat} at acidic pH. The Cys630 mutant exhibited the same behavior as the mutants of Asp675 and Ser457 in the basic limb of the pH profile displaying a shift to higher $\text{p}K_a$.⁶¹ In general, an increase of the basic $\text{p}K_a$ and a decreased catalytic activity were observed in all mutants. Shen *et al.* suggested that the shift may arise from a change in the rate-limiting step from the pH-dependent step to the hydride transfer step. As a candidate responsible for the acidic $\text{p}K_a$, the N1 atom of FAD was proposed. The origin of the basic $\text{p}K_a$ was not clarified.

According to our proposal, Asp675 could be responsible for the basic $\text{p}K_a$ value of the pH dependence of k_{cat} . To investigate this possibility, we studied the influence of Cys630 and Ser457 on the titration behavior of Asp675. As shown in Table I, the S457A mutant form of CPR remarkably lowers the protonation energy of the aspartate at pH 7 by about 5 kcal mol⁻¹ leading to a more stable protonation of the site. Also, the mutation on the C630A lowers the protonation energy of the aspartate by almost 2 kcal mol⁻¹ at pH 7. The energy contribution responsible for the change is ΔG_{back} (Table I). The fact that mutations on the C630A or S457A do not affect cofactor binding (NADP⁺ or NADPH) to CPR⁶¹ could be rationalized on the basis of the carboxylic acid's charge, in which the residue is always protonated for the different forms of the enzyme. Thus, our results are in full agreement with the experimental data in Ref. 61. The catalytic model proposed in Ref. 61 suggests that Cys630 acts as proton donor.

Nevertheless, the experimental results therein do not rule out that Asp675 is responsible for the basic $\text{p}K_a$ value of 9.6 and that the other two residues influence its titration behavior by shifting the protonation energy to even higher values. Most likely, because the hypothesis that an aspartate could have a $\text{p}K_a$ of about 9.5 is counterintuitive, the authors proposed a model, in which the cysteine residue is able to deprotonate and then to act as a proton donor. However, our results fit perfectly to their data and suggest not only that Asp675 would be protonated because of its low protonation energy but also how the cysteine and serine residues influence its titration behavior. Instead, according to our calculations, Cys630 does not titrate in the analyzed pH range, neither for wild-type CPR nor for S475A CPR model. At pH 7, the energy required to deprotonate Cys630 is -18.3 kcal mol⁻¹ for native enzyme and -17.3 kcal mol⁻¹ for the S475A mutant form. Such a low protonation energy for Cys630 is caused by the hydrophobic environment around the cysteine when it is buried in the protein. Hence, according to our results, Asp675 can act as a proton donor in CPR and thus has an important function during the catalytic cycle.

CONCLUSION

When studying a protein system at molecular level, it is often believed that aminoacid residues behave like their free version aminoacids in aqueous solution. Thus, it is common to assume that carboxylic residues in a protein are negatively charged and basic residues are positively charged. This work shows that aminoacids in proteins can have a quite different titration behavior from free aminoacids, even in structurally related polypeptides. Through electrostatic calculations, we determined a particular feature that completely distinguishes two groups of enzymes, which at first glance, look structurally alike. The different degrees of solvent exposure of the carboxylic acid in the active site of flavin and diflavin reductases lead to different titration properties of this residue. In bacterial FPRs and diflavin reductases, the active site carboxylic acid is buried in the protein, which indicates that this residue is protonated at pH 7. On the other hand, in plastidic FNRs the active site carboxylic acid is exposed to the solvent and is deprotonated at neutral pH.

All enzymes investigated in this study catalyze the same reaction, but the direction of the physiological reaction depends on the metabolic route that the protein is part of. Bacterial FPRs and diflavin reductases take up electrons from NADPH, whereas plastidic FNRs transfer electrons from reduced Fd to NADP⁺. A negatively carboxylic acid present in FNRs may help positioning NADP⁺ appropriately for transferring the hydride from the flavin ring of the enzyme to NADP⁺. Hence, the negative charge on the glutamic acid residue in FNRs favors NADP⁺ binding. The lack of charge on the equivalent

residue in FPRs and diflavin reductases disfavors NADP⁺ over NADPH binding. It is plausible that the protonation behavior of this active site carboxylic acid is a feature tuned by evolution to recruit these enzymes into different metabolic pathways.

ACKNOWLEDGMENTS

V.I.D. received a fellowship from the DAAD for her stay in Germany. V.I.D. is a fellow of CONICET, and N.C. is a staff member of the same institution. The authors are grateful to R. Thomas Ullmann for carefully reading the manuscript.

REFERENCES

- Carrillo N, Ceccarelli EA. Open questions in ferredoxin-NADP⁺ reductase catalytic mechanism. *Eur J Biochem* 2003;270:1900–1915.
- Spiegelhauer O, Dickert F, Mende S, Niks D, Hille R, Ullmann M, Dobbek H. Kinetic characterization of xenobiotic reductase A from *Pseudomonas putida* 86. *Biochemistry* 2009;48:11412–11420.
- Paine MJ, Garner AP, Powell D, Sibbald J, Sales M, Pratt N, Smith T, Tew DG, Wolf CR. Cloning and characterization of a novel human dual flavin reductase. *J Biol Chem* 2000;275:1471–1478.
- Porter TD, Kasper CB. NADPH-cytochrome P-450 oxidoreductase: flavin mononucleotide and flavin adenine dinucleotide domains evolved from different flavoproteins. *Biochemistry* 1986;25:1682–1687.
- Porter TD. An unusual yet strongly conserved flavoprotein reductase in bacteria and mammals. *Trends Biochem Sci* 1991;16:154–158.
- Murataliev MB, Feyereisen R, Walker FA. Electron transfer by diflavin reductases. *Biochim Biophys Acta* 2004;1698:1–26.
- Portal P, Villamil SF, Alonso GD, De Vas MG, Flawiá MM, Torres HN, Paveto C. Multiple NADPH-cytochrome P450 reductases from *Trypanosoma cruzi* suggested role on drug resistance. *Mol Biochem Parasitol* 2008;160:42–51.
- Garcin ED, Bruns CM, Lloyd SJ, Hosfield DJ, Tiso M, Gachhui R, Stuehr DJ, Tainer JA, Getzoff ED. Structural basis for isozyme-specific regulation of electron transfer in nitric-oxide synthase. *J Biol Chem* 2004;279:37918–37927.
- Zhang W, Braun A, Bauman Z, Olteanu H, Madzalan P, Banerjee R. Expression profiling of homocysteine junction enzymes in the NCI60 panel of human cancer cell lines. *Cancer Res* 2005;65:1554–1560.
- Shatsky M, Nussinov R, Wolfson HJ. A method for simultaneous alignment of multiple protein structures. *Proteins* 2004;56:143–156.
- Humphrey W, Dalke A, Schulten K. VMD: visual molecular dynamics. *J Mol Graph* 1996;14:33–38.
- Holm L, Kääräinen S, Rosenström P, Schenkel A. Searching protein structure databases with DaliLite v.3. *Bioinformatics* 2008;24: 2780–2781.
- Wang M, Roberts DL, Paschke R, Shea TM, Masters BS, Kim JJ. Three-dimensional structure of NADPH-cytochrome P450 reductase: prototype for FMN- and FAD-containing enzymes. *Proc Natl Acad Sci USA* 1997;94:8411–8416.
- Lamb DC, Kim Y, Yermalitskaya LV, Yermalitsky VN, Lepesheva GI, Kelly SL, Waterman MR, Podust LM. A second FMN binding site in yeast NADPH-cytochrome P450 reductase suggests a mechanism of electron transfer by diflavin reductases. *Structure* 2006;14:51–61.
- Zhang J, Martásek P, Paschke R, Shea T, Siler Masters BS, Kim JJ. Crystal structure of the FAD/NADPH-binding domain of rat neuronal nitric-oxide synthase. Comparisons with NADPH-cytochrome P450 oxidoreductase. *J Biol Chem* 2001;276:37506–37513.
- Wolthers KR, Lou X, Toogood HS, Leys D, Scrutton NS. Mechanism of coenzyme binding to human methionine synthase reductase revealed through the crystal structure of the FNR-like module and isothermal titration calorimetry. *Biochemistry* 2007;46:11833–11844.
- Gruez A, Pignol D, Zeghouf M, Covès J, Fontecave M, Ferrer JL, Fontecilla-Camps JC. Four crystal structures of the 60 kDa flavoprotein monomer of the sulfite reductase indicate a disordered flavodoxin-like module. *J Mol Biol* 2000;299:199–212.
- Deng Z, Aliverti A, Zanetti G, Arakaki AK, Ottado J, Orellano EG, Calcaterra NB, Ceccarelli EA, Carrillo N, Karplus PA. A productive NADP⁺ binding mode of ferredoxin-NADP⁺ reductase revealed by protein engineering and crystallographic studies. *Nat Struct Biol* 1999;6:847–853.
- Bruns CM, Karplus PA. Refined crystal structure of spinach ferredoxin reductase at 1.7 Å resolution: oxidized, reduced and 2'-phospho-5'-AMP bound states. *J Mol Biol* 1995;247:125–145.
- Dorowski A, Hofmann A, Steegborn C, Boicu M, Huber R. Crystal structure of paprika ferredoxin-NADP⁺ reductase. Implications for the electron transfer pathway. *J Biol Chem* 2001;276:9253–9263.
- Serre L, Vellieux FM, Medina M, Gomez-Moreno C, Fontecilla-Camps JC, Frey M. X-ray structure of the ferredoxin:NADP⁺ reductase from the cyanobacterium *Anabaena* PCC 7119 at 1.8 Å resolution, and crystallographic studies of NADP⁺ binding at 2.25 Å resolution. *J Mol Biol* 1996;263:20–39.
- Kurisu G, Kusunoki M, Katoh E, Yamazaki T, Teshima K, Onda Y, Kimata-Aruga Y, Hase T. Structure of the electron transfer complex between ferredoxin and ferredoxin-NADP(+) reductase. *Nat Struct Biol* 2001;8:117–121.
- Aliverti A, Faber R, Finnerty CM, Ferioli C, Pandini V, Negri A, Karplus PA, Zanetti G. Biochemical and crystallographic characterization of ferredoxin-NADP(+) reductase from nonphotosynthetic tissues. *Biochemistry* 2001;40:14501–14508.
- Nascimento AS, Catalano-Dupuy DL, Bernardes A, Neto MdeO, Santos MA, Ceccarelli EA, Polikarpov I. Crystal structures of *Leptospira interrogans* FAD-containing ferredoxin-NADP⁺ reductase and its complex with NADP⁺. *BMC Struct Biol* 2007;7:69–69.
- Milani M, Balconi E, Aliverti A, Mastrangelo E, Seeber F, Bolognesi M, Zanetti G. Ferredoxin-NADP⁺ reductase from *Plasmodium falciparum* undergoes NADP⁺-dependent dimerization and inactivation: functional and crystallographic analysis. *J Mol Biol* 2007;367: 501–513.
- Karlsson A, Beharry ZM, Matthew Eby D, Coulter ED, Neidle EL, Kurtz DM, Eklund H, Ramaswamy S. X-ray crystal structure of benzoate 1,2-dioxygenase reductase from *Acinetobacter* sp. strain ADP1. *J Mol Biol* 2002;318:261–272.
- Ingelman M, Bianchi V, Eklund H. The three-dimensional structure of flavodoxin reductase from *Escherichia coli* at 1.7 Å resolution. *J Mol Biol* 1997;268:147–157.
- Sridhar Prasad G, Kresge N, Muhlberg AB, Shaw A, Jung YS, Burgess BK, Stout CD. The crystal structure of NADPH:ferredoxin reductase from *Azotobacter vinelandii*. *Protein Sci* 1998;7:2541–2549.
- Correll CC, Batie CJ, Ballou DP, Ludwig ML. Phthalate dioxygenase reductase: a modular structure for electron transfer from pyridine nucleotides to [2Fe-2S]. *Science* 1992;258:1604–1610.
- Wang A, Zeng Y, Han H, Weeratunga S, Morgan BN, Moënnelocoz P, Schönbrunn E, Rivera M. Biochemical and structural characterization of *Pseudomonas aeruginosa* Bfd and FPR: ferredoxin NADP⁺ reductase and not ferredoxin is the redox partner of heme oxygenase under iron-starvation conditions. *Biochemistry* 2007;46: 12198–12211.
- Nogués I, Pérez-Dorado I, Frago S, Bittel C, Mayhew SG, Gómez-Moreno C, Hermoso JA, Medina M, Cortez N, Carrillo N. The ferredoxin-NADP(H) reductase from *Rhodobacter capsulatus*: molecular structure and catalytic mechanism. *Biochemistry* 2005;44: 11730–11740.
- Brünger AT, Karplus M. Polar hydrogen positions in proteins: empirical energy placement and neutron diffraction comparison. *Proteins* 1988;4:148–156.
- Brooks BR, Brucoleri RE, Olafson BD, States DJ, Swaminathan S, Karplus M. CHARMM: A program for macromolecular energy, minimization, and dynamics calculations. *J Comput Chem* 1983;4:187–217.

34. Dumit VI, Essigke T, Cortez N, Ullmann GM. Mechanistic insights into ferredoxin-NADP(H) reductase catalysis involving the conserved glutamate in the active site. *J Mol Biol* 2010;397:814–825.
35. Ullmann GM, Knapp EW. Electrostatic models for computing protonation and redox equilibria in proteins. *Eur Biophys J* 1999;28:533–551.
36. Essigke T. A continuum electrostatic approach for calculating the binding energetics of multiple ligands, PhD Thesis. Bayreuth, Germany: University of Bayreuth, 2008. Available at: <http://opus.ub.uni-bayreuth.de/volltexte/2008/410/>.
37. Ullmann GM. Relations between protonation constants and titration curves in polyprotic acids: a critical view. *J Phys Chem B* 2003;107:1263–1271.
38. Klingen AR, Bombarda E, Ullmann GM. Theoretical investigation of the behavior of titratable groups in proteins. *Photochem Photobiol Sci* 2006;5:588–596.
39. Homeyer N, Essigke T, Ullmann GM, Sticht H. Effects of histidine protonation and phosphorylation on histidine-containing phosphocarrier protein structure, dynamics, and physicochemical properties. *Biochemistry* 2007;46:12314–12326.
40. Bombarda E, Ullmann GM. pH-dependent pKa values in proteins—A theoretical analysis of protonation energies with practical consequences for enzymatic reactions. *J Phys Chem B* 2010;114:1994–2003.
41. Tanford C, Roxby R. Interpretation of protein titration curves. application to lysozyme. *Biochemistry* 1972;11:2192–2198.
42. Bashford D, Karplus M. Multiple-site titration curves of proteins: an analysis of exact and approximate methods for their calculations. *J Phys Chem* 1991;95:9557–9561.
43. Bashford D, Karplus M. pKa's of ionizable groups in proteins: atomic detail from a continuum electrostatic model. *Biochemistry* 1990;29:10219–10225.
44. Taly A, Sebban P, Smith JC, Ullmann GM. The structural changes in the Q_B pocket of the photosynthetic reaction center depend on pH: a theoretical analysis of the proton uptake upon Q_B reduction. *Biophys J* 2003;84:2090–2098.
45. Calimet N, Ullmann GM. The influence of a transmembrane pH gradient on protonation probabilities of bacteriorhodopsin: the structural basis of the back-pressure effect. *J Mol Biol* 2004;339:571–589.
46. Becker T, Ullmann RT, Ullmann GM. Simulation of the electron transfer between the tetraheme-subunit and the special pair of the photosynthetic reaction center using a microstate description. *J Phys Chem B* 2007;111:2957–2968.
47. Bombarda E, Becker T, Ullmann GM. Influence of the membrane potential on the protonation of bacteriorhodopsin: insights from electrostatic calculations into the regulation of proton pumping. *J Am Chem Soc* 2006;128:12129–12139.
48. Bombarda E, Ullmann GM. Continuum electrostatic investigations of charge transfer processes in biological molecules using a microstate description. *Faraday Disc* 2011;148:173–193.
49. Kim J, Mao J, Gunner MR. Are acidic and basic groups in buried proteins predicted to be ionized? *J Mol Biol* 2005;348:1283–1298.
50. Song YF, Gunner MR. Using multiconformation continuum electrostatics to compare chloride binding motifs in alpha-amylase, human serum albumin, and Omp32. *J Mol Biol* 2009;387:840–856.
51. Zhang J, Gunner MR. Multiconformation continuum electrostatics analysis of the effects of a buried asp introduced near heme a in rhodobacter sphaeroides cytochrome c oxidase. *Biochemistry* 2010;49:8043–8052.
52. Beroza P, Fredkin DR, Okamura MY, Feher G. Protonation of interacting residues in a protein by a Monte Carlo method: application to lysozyme and the photosynthetic reaction center of rhodobacter sphaeroides. *Proc Natl Acad Sci USA* 1991;88:5804–5808.
53. Medina M, Martínez-Júlvez M, Hurley JK, Tollin G, Gómez-Moreno C. Involvement of glutamic acid 301 in the catalytic mechanism of ferredoxin-NADP⁺ reductase from *Anabaena* PCC 7119. *Biochemistry* 1998;37:2715–2728.
54. Aliverti A, Deng Z, Ravasi D, Piubelli L, Karplus PA, Zanetti G. Probing the function of the invariant glutamyl residue 312 in spinach ferredoxin-NADP⁺ reductase. *J Biol Chem* 1998;273:34008–34015.
55. Razquin P, Fillat MF, Schmitz S, Stricker O, Böhme H, Gómez-Moreno C, Peleato ML. Expression of ferredoxin-NADP⁺ reductase in heterocysts from *Anabaena* sp. *Biochem J* 1996;316:157–160.
56. Ceccarelli EA, Arakaki AK, Cortez N, Carrillo N. Functional plasticity and catalytic efficiency in plant and bacterial ferredoxin-NADP(H) reductases. *Biochim Biophys Acta* 2004;1698:155–165.
57. Hubbard PA, Shen AL, Paschke R, Kasper CB, Kim JJ. NADPH-cytochrome P450 oxidoreductase. Structural basis for hydride and electron transfer. *J Biol Chem* 2001;276:29163–29170.
58. Tejero J, Martínez-Julvez M, Mayoral T, Luquita A, Sanz-Aparicio J, Hermoso JA, Hurley JK, Tollin G, Gómez-Moreno C, Medina M. Involvement of the pyrophosphate and the 2'-phosphate binding regions of ferredoxin-NADP⁺ reductase in coenzyme specificity. *J Biol Chem* 2003;278:49203–49214.
59. Piubelli L, Aliverti A, Arakaki AK, Carrillo N, Ceccarelli EA, Karplus PA, Zanetti G. Competition between C-terminal tyrosine and nicotinamide modulates pyridine nucleotide affinity and specificity in plant ferredoxin-NADP(+) reductase. *J Biol Chem* 2000;275:10472–10476.
60. Bortolotti A, Pérez-Dorado I, Goñi G, Medina M, Hermoso JA, Carrillo N, Cortez N. Coenzyme binding and hydride transfer in *Rhodobacter capsulatus* ferredoxin/ flavodoxin NADP(H) oxidoreductase. *Biochim Biophys Acta* 2009;1794:199–210.
61. Shen AL, Sem DS, Kasper CB. Mechanistic studies on the reductive half-reaction of NADPH-cytochrome P450 oxidoreductase. *J Biol Chem* 1999;274:5391–5398.
62. Lanyi JK. Bacteriorhodopsin as a model for proton pumps. *Nature* 1995;375:461–463.
63. Paddock ML, Feher G, Okamura MY. Proton transfer pathways and mechanism in bacterial reaction centers. *FEBS Lett* 2003;555:45–50.
64. Michel H, Behr J, Harrenga A, Kannt A. Cytochrome c oxidase: structure and spectroscopy. *Annu Rev Biophys Biomol Struct* 1998;27:329–356.